Magnetic and magnetocaloric properties of $Pr_{2-x}Nd_xFe_{17}$ ribbons

Cite as: AIP Advances 9, 035211 (2019); doi: 10.1063/1.5080105
Presented: 15 January 2019 • Submitted: 5 November 2018 •
Accepted: 16 December 2018 • Published Online: 11 March 2019

Bishnu Dahal,[1] Parashu Kharel,[1,2,a)] Thomas Ott,[1,2] Wenyong Zhang,[2,3] Shah Valloppilly,[2] Ralph Skomski,[2,3] and David Sellmyer[2,3]

AFFILIATIONS

[1]Department of Physics, South Dakota State University, Brookings, South Dakota 57007, USA
[2]Nebraska Center for Materials and Nanoscience, University of Nebraska, Lincoln, Nebraska 68588, USA
[3]Department of Physics and Astronomy, University of Nebraska, Lincoln, Nebraska 68588, USA

Note: This paper was presented at the 2019 Joint MMM-Intermag Conference.
[a)]parashu.kharel@sdstate.edu

ABSTRACT

The structural, magnetic and magnetocaloric properties of Fe deficient $Pr_{2-x}Nd_xFe_{17}$ (x = 0.5, 0.7) alloys prepared by arc-melting and melt-spinning have been investigated. The room temperature x-ray diffraction patterns show that the samples are nearly single-phase and crystallize in the rhombohedral Th_2Zn_{17}-type crystal structure. The Curie temperatures determined from the thermomagnetic curves are 302 K and 307 K for $Pr_{1.5}Nd_{0.5}Fe_{17}$ and $Pr_{1.3}Nd_{0.7}Fe_{17}$, respectively. The peak magnetic entropy change and the relative cooling power at field change of 50 kOe are 3.01 J/kgK and 345 J/kg for $Pr_{1.5}Nd_{0.5}Fe_{17}$, and 4.31 J/kgK and 487 J/kg for $Pr_{1.3}Nd_{0.7}Fe_{17}$, respectively. The absence of magnetic and thermal hysteresis with relatively high cooling efficiency suggests that the alloys have potential for magnetic refrigeration.

I. INTRODUCTION

Magnetic refrigeration is expected to become an alternative to the current gas-compression cooling system with advantages such as high energy efficiency, low manufacturing and maintenance costs, and use of environment friendly solid state materials.[1–6] The magnetic refrigeration (MR) is based on the magnetocaloric effect (MCE), where a magnetic material shows thermal response to an external magnetic field.[7] The MCE is measured either in terms of the magnetic entropy change (ΔS_M) in an isothermal process or in terms of the temperature change (ΔT_{ad}) in an adiabatic process. Therefore, development of magnetic materials with large ΔS_M and ΔT_{ad} over a broad temperature range near room temperature is crucial for the advancement of magnetic refrigeration technology.[8]

The value of ΔS_M depends on the rate at which magnetization changes with temperature ($\partial M/\partial T$). Therefore, large values of ΔS_M are obtained near phase transitions. Materials undergoing magnetostructural phase transitions (first-order phase transition FOPT), such as Gd-Si-Ge,[9] La-Fe-Si,[10] Mn-Fe-P-As,[11] and Ni-Mn-based Heusler alloys[12] exhibit very large values of ΔS_M near room temperature due to sharp changes in magnetizations. However, materials undergoing FOPT are not considered ideal for magnetic refrigeration because of large magnetic and thermal hysteresis, narrow operating temperature range, irreversibility in entropy and temperature changes over magnetization/demagnetization cycles, and issues with mechanical stability.[13] Most of these issues can be addressed by using materials that show second-order phase transitions (SOPT) as magnetic refrigerants, but they exhibit relatively lower values of ΔS_M. Among SOPT materials, elemental gadolinium (Gd) combines moderate value of ΔS_M with relatively high cooling efficiency but it is expensive and highly susceptible to oxidation.[3] Other SOPT materials yielding entropy changes comparable to Gd are R_2Fe_{17}-type (R = rare-earth element) alloys[14] which contain much smaller amounts of expensive rare earths. Our focus is on the Curie temperatures T_C of these alloys, which can be fine-tuned by adjusting the elemental composition, especially through the choice of rare-earth combinations.

Here we investigate the structural, magnetic and magnetocaloric properties of Fe deficient $Pr_{2-x}Nd_xFe_{17}$ (x = 0.5, 0.7)

alloys synthesized in the form of ribbons. Our goal is to develop intermediate compositions with Curie temperature very close to room temperature, starting from Pr_2Fe_{17}[15] and Nd_2Fe_{17}.[16,17] Since the T_c of Pr_2Fe_{17} is somewhat lower than room temperature (283 K) and that of Nd_2Fe_{17} is somewhat higher than room temperature (340 K), it is possible to adjust the T_c of $Pr_{2-x}Nd_xFe_{17}$ near room temperature by adjusting the elemental composition. We have found that the Fe deficient $Pr_{1.3}Nd_{0.7}Fe_{17}$ alloy maintains high magnetization with a T_c of 307 K. In addition to choosing a combination of Pr and Nd as the rare-earths to tune T_c, our experimental investigations suggested that slightly Fe-deficient composition facilitated better phase purity and slightly higher net magnetization in comparison to $(Pr,Nd)_2Fe_{17}$ counterparts, and will be beneficial for the magnetocaloric properties.

II. EXPERIMENTAL METHODS

The Fe deficient $Pr_{2-x}Nd_xFe_{17}$ (x = 0.5, 0.7) alloys in the form of ribbons were synthesized using arc-melting, followed by rapid quenching in a melt-spinner. First, pieces of Pr, Nd, and Fe with proper weight ratio were cut from commercially available pellets and then melted on a Cu hearth of an arc-melting furnace in a highly pure argon environment. The arc-melted ingots were broken into pieces, induction melted in a quartz tube inside a melt-spinner chamber and rapidly quenched onto the surface of a copper wheel rotating at 25 m/s. The phase formation and structural properties of the samples were investigated using powder x-ray diffraction (XRD) using a PANalytical Empyrean Diffractometer with Cu Kα radiation (wavelength of 1.5418 Å). The XRD patterns were analyzed by Rietveld method using TOPAS software (Bruker, AXS). The magnetic properties were investigated using Quantum Design VersaLab magnetometer and Physical Property Measurement System (PPMS). The estimated elemental compositions were confirmed using energy-dispersive x-ray spectroscopy (EDX) in a FEI Nova NanoSEM450.

III. RESULTS AND DISCUSSION

Figure 1 shows the XRD patterns of the rapidly quenched $Pr_{1.3}Nd_{0.7}Fe_{17}$ and $Pr_{1.5}Nd_{0.5}Fe_{17}$ ribbons measured at room temperature. In order to determine the lattice parameters and the presence of secondary phase, the experimental XRD patterns were compared with the simulated patterns by Rietveld refinement method using TOPAS software. The powder x-ray diffraction simulations indicate that the compounds are formed nearly single phase with Th_2Zn_{17}-type rohombohedral crystal structure ($R\bar{3}m$ space group). Traces of upto 5 wt. % of α-Fe impurity was detected in the phase analysis by Rietveld method. The lattice parameters are: a = 8.579 Å, c = 12.486 Å and a = 8.575 Å, c = 12.499 Å, respectively for x = 0.5 and 0.7, thus indicating only a minor cell expansion along the c-axis in the Nd-rich sample. In the Th_2Zn_{17}-type structure, Pr and Nd share the Wyckoff position *6c* (0, 0, 0.333), whereas Fe is distributed among sites *6c* (0, 0, 0.097), *9d* (0.5, 0, 0.5), *18f* (0.333, 0, 0) and *18h* (0.5, 0.5, 0.167). The elemetal compositions determined using EDX spectroscopy are $Pr_{1.3}Nd_{0.7}Fe_{15}$ and $Pr_{1.5}Nd_{0.5}Fe_{15}$ and therefore we investigated the Fe-deficiency in the diffraction profile analysis. The analysis suggests that *6c* and *18f* sites are the Fe-lean sites and the composition based on this analysis matches closely with the nominal composition obtained by EDX spectroscopy.

Figure 2 shows the thermomagnetic curves $M(T)$ of the $Pr_{2-x}Nd_xFe_{17}$ ribbons measured at 1 kOe. For these measurements, the ribbons were first cooled to 100 K at H = 0 and measurements were performed at 1 kOe while the temperature increased from 100 to 380 K at 2 K/min (zero field cool measurement).

The $M(T)$ curves are smooth and show a SOPT from a ferromagnetic to a paramagnetic phase. No thermal hysteresis was observed when the measurement was reversed from 380 K to 100 K (not shown). The Curie temperatures obtained from the peak values of $\frac{dM}{dT}$ *vs.* T curves are 302 K for $Pr_{1.5}Nd_{0.5}Fe_{17}$ and 307 K for $Pr_{1.3}Nd_{0.7}Fe_{17}$. For example, the $\frac{dM}{dT}$ *vs.* T curve of $Pr_{1.3}Nd_{0.7}Fe_{17}$ is shown as the inset of Fig. 2.

Figures 3(a) and 3(c) show the isothermal magnetization curves of $Pr_{1.3}Nd_{0.7}Fe_{17}$ and $Pr_{1.5}Nd_{0.5}Fe_{17}$ recorded at various temperatures between 260 K and 380 K, and the corresponding H/M versus M^2 curves (Arrott plot) are shown in Figs. 3(b) and 3(d), respectively. The Arrott plot can be used to determine the Curie temperature and also to identify the nature of the phase transition. According to the Banerjee criterion,[18] positive slope of H/M versus M^2 curves indicates a SOPT whereas the negative slope indicates a

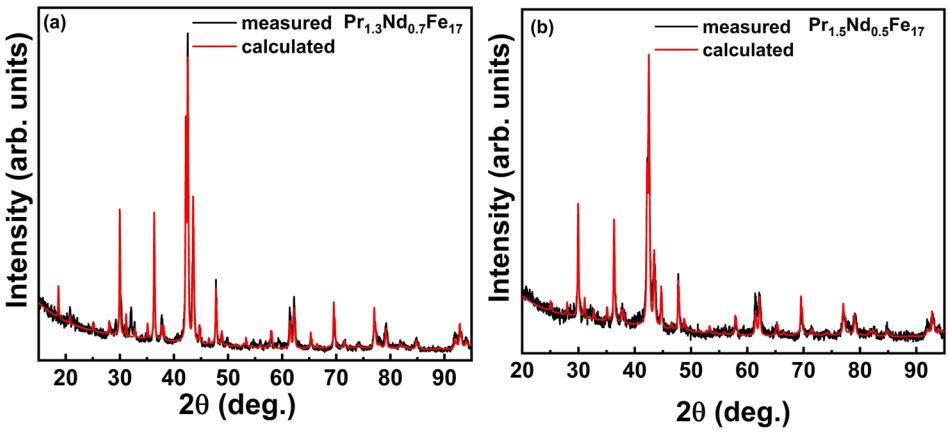

FIG. 1. Powder x-ray diffraction pattern of experimental and the simulation data from the Rietveld analysis (a) $Pr_{1.3}Nd_{0.7}Fe_{17}$ and (b) $Pr_{1.5}Nd_{0.5}Fe_{17}$.

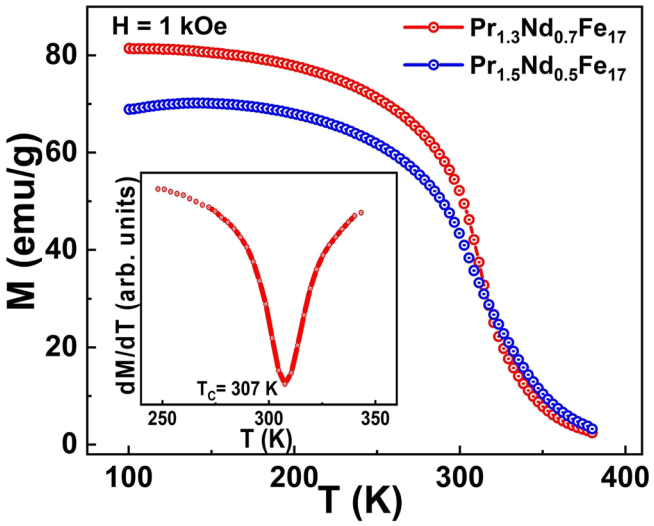

FIG. 2. Temperature dependence of magnetization of $Pr_{2-x}Nd_xFe_{17}$ ribbons measured at 1 kOe field. The inset shows *dM/dT vs. T* of $Pr_{1.3}Nd_{0.7}Fe_{17}$, which is used to determine the Curie temperature.

FOPT. In our case, as shown in Figs. 3(b) and 3(d), all the curves show a positive slope confirming SOPT for both $Pr_{1.3}Nd_{0.7}Fe_{17}$ and $Pr_{1.5}Nd_{0.5}Fe_{17}$ ribbons.

We have investigated the magnetocaloric properties of $Pr_{2-x}Nd_xFe_{17}$ (x = 0.5, 0.7) ribbons in terms ΔS_M and relative cooling power (RCP). In order to determine ΔS_M for the ribbons, we recorded isothermal magnetization curves between 0 and 50 kOe, at various temperatures near their Curie temperatures. The *M(H)* curves recorded for $Pr_{1.3}Nd_{0.7}Fe_{17}$ and $Pr_{1.5}Nd_{0.5}Fe_{17}$ at various temperature intervals (2 K, 5 K, and 10 K) starting from 2 K near T_C are shown in Figs. 3(a) and 3(c), respectively. The entropy changes ΔS_M at various temperatures were obtained using Maxwell's thermodynamic relation $S_M(T,H) = \int_0^H \left(\frac{dM}{dT}\right)_H dH$ utilizing the *M(H)* data. Figures 4(a) and 4(b) show the entropy changes ΔS_M as a function of temperature. The peak values of magnetic entropy change $\Delta S_{M,max}$ at magnetic field change of 50 kOe are 4.31 $Jkg^{-1}K^{-1}$ and 3.01 $Jkg^{-1}K^{-1}$ for $Pr_{1.3}Nd_{0.7}Fe_{17}$ and $Pr_{1.5}Nd_{0.5}Fe_{17}$ alloys, respectively. These values are comparable to those in other Fe-rich rare-earth intermetallics[14] while the adjusted Curie temperature near 300 K is highly beneficial for room-temperature magnetic refrigeration. Note that R_2Fe_{17} alloys are expected to have similar peak entropies across the lanthanide series, because the relatively weak rare-earth iron intersublattice exchange[19] strongly reduces the rare-earth entropy change near the Curie temperature. By contrast, the Curie temperature increases systematically towards the middle of the lanthanide series (476 K for Gd_2Fe_{17}).

From a practical viewpoint, the cooling efficiency of a magnetocaloric material is parameterized by the relative cooling power (RCP). The RCP measures the amount of heat transferred from a hot reservoir to cold reservoir in a thermodynamic cycle. The insets of Figs. 4(a) and 4(b) show the RCP values of $Pr_{1.3}Nd_{0.7}Fe_{17}$ and

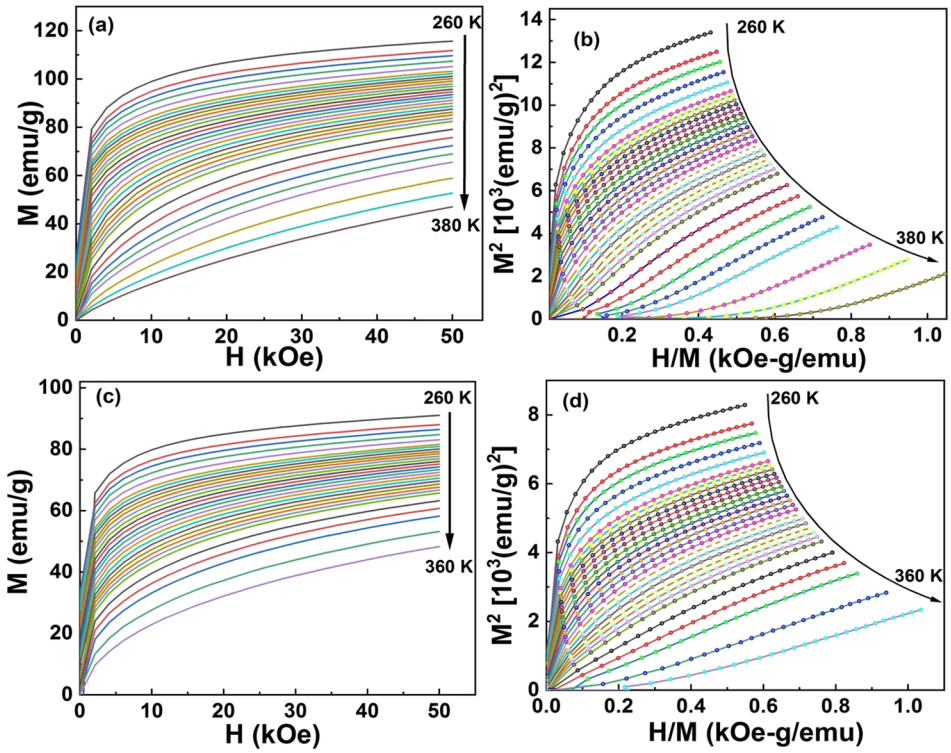

FIG. 3. The isothermal magnetization curves measured at different temperatures, and the corresponding M^2 *vs.* H/M curves (Arrott Plot) for $Pr_{1.3}Nd_{0.7}Fe_{17}$ alloy (a and b) and for $Pr_{1.5}Nd_{0.5}Fe_{17}$ alloy (c and d), respectively.

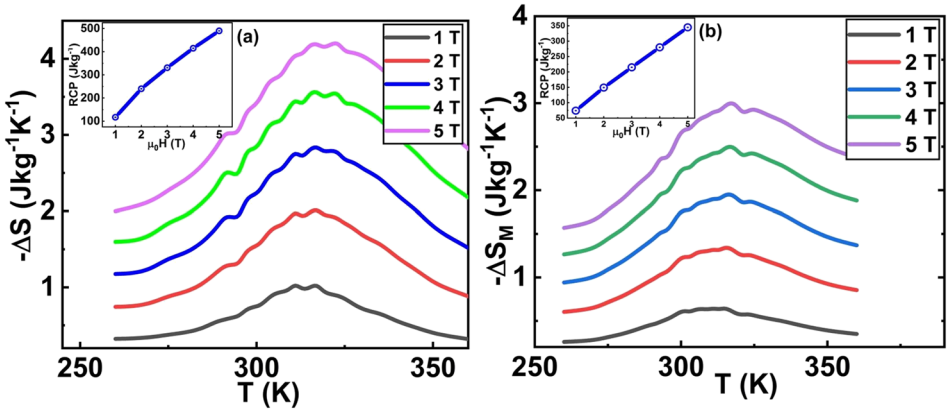

FIG. 4. Magnetic entropy change as a function of temperature for (a) $Pr_{1.3}Nd_{0.7}Fe_{17}$ and (b) $Pr_{1.5}Nd_{0.5}Fe_{17}$. The insets show the RCP as a function of $\mu_0 H$.

$Pr_{1.5}Nd_{0.5}Fe_{17}$ ribbons at various magnetic fields, respectively. These RCP values were calculated using the expression $RCP = |\Delta S_{M,max}| \times \Delta T_{FWHM}$, where ΔT_{FWHM} is the full width at half maximum of $\Delta S_M(T)$ curve. The RCP values for $Pr_{1.3}Nd_{0.7}Fe_{17}$ and $Pr_{1.5}Nd_{0.5}Fe_{17}$ ribbons at field changes of 50 kOe are 487 and 345 Jkg^{-1}, respectively. Although both $Pr_{1.5}Nd_{0.5}Fe_{17}$ and $Pr_{1.3}Nd_{0.7}Fe_{17}$ have modest values of $\Delta S_{M,max}$, the RCP values are larger, mainly due to their broad $\Delta S_M(T)$ curve. While the ΔS_M values are comparable to that of other materials showing SOPT near room temperature, the values of RCP in our samples are significantly higher.[2,3,20]

IV. CONCLUSIONS

In summary, we have prepared Fe deficient $Pr_{1.3}Nd_{0.7}Fe_{17}$ and $Pr_{1.5}Nd_{0.5}Fe_{17}$ alloys using arc-melting and melt-spinning. The x-ray diffraction analysis show that both alloys crystallized in the rhombohedral Th_2Zn_{17}-type structure. The peak magnetic entropy changes of 3.01 J/kgK in $Pr_{1.5}Nd_{0.5}Fe_{17}$ and 4.31 J/kgK in $Pr_{1.3}Nd_{0.7}Fe_{15}$ are comparable to those of other materials with second-order phase transitions and the respective Curie temperatures, 302 K and 307 K, are very close to room temperature. Furthermore, a relatively high cooling power of 487 J/kg has been achieved in $Pr_{1.3}Nd_{0.7}Fe_{17}$. The peak entropy change, the cooling power, the operation near room temperature, and the relatively low raw-materials price make the alloys potential candidates for room-temperature magnetic refrigerants.

ACKNOWLEDGMENTS

This research was supported by NSF, DMR under Award DMREF: SusChEM 1436385. The work was performed in part in the Nebraska Nanoscale Facility, Nebraska Center for Materials and Nanoscience, which is supported by the National Science Foundation under Award ECCS: 1542182, and the Nebraska Research Initiative.

REFERENCES

[1] V. K. Pecharsky and K. A. Gschneidner, J. Magn. Magn. **200**, 44–56 (1999).
[2] V. Franco, J. S. Blázquez, B. Ingale, and A. Conde, Annu. Rev. Mater Res. **42**, 305–342 (2012).
[3] M. H. Phan and S. C. Yub, J. Magn. Magn. Mater **308**, 325–340 (2007).
[4] A. Tishin and Y. Spichkin, *The Magnetocaloric Effect and its Applications* (CRC Press, Boca Raton, 2003).
[5] B. R. Dahal, K. Schroeder, M. M. Allyn, R. Tackett, Y. Huh, and P. Kharel, Mater. Res. Express **5**, 106103 (2018).
[6] S. Pandey, A. Quetz, I. D. Rodionov, A. Aryal, M. I. Blinov, I. S. Titov, V. N. Prudnikov, A. B. Granovsky, I. Dubenko, S. Stadler, and N. Ali, J. Appl. Phys. **117**, 183905 (2015).
[7] N. A. de Oliveira and P. J. von Ranke, Phys. Reports **489**, 89–149 (2010).
[8] J. Liu, T. Gottschall1, K. P. Skokov, J. D. Moore, and O. Gutfleisch, Nature Mater. **11**, 620–626 (2012).
[9] V. K. Pecharsky and K. A. Gschneidner, Phy. Rev. Lett. **78**, 4494 (1997).
[10] A. Fujita, S. Fujieda, Y. Hasegawa, and K. Fukamichi, Phys. Rev. B **67**, 104416 (2003).
[11] O. Tegus, E. Bruck, K. H. J. Buschow, and F. R. de Boer, Nature **415**, 150 (2002).
[12] I. Dubenko, M. Khan, A. K. Pathak, B. R. Gautam, S. Stadler, and N. Ali, J. Magn. Magn. Mater. **321**, 754 (2009).
[13] V. Franco, J. S. Blázquez, and A. Conde, Appl. Phys. Lett. **89**, 222512 (2006).
[14] K. Mandal, A. Yan, P. Kerschl, A. Handstein, O. Gutfleisch, and K.-H. Müller, J Phys D: Appl Phys. **37**, 2628 (2004).
[15] L. M. Levinson, E. Rosenberg, A. Shaulov, S. Shtrikman, and K. Strnat, J. Appl. Phys **41**, 910 (1970).
[16] P. Alvareza, J. Sánchez-Marcos, J. L. Sanchez Llamazares, V. Francod, M. Reiffers, J. A. Blanco, and P. Gorria, Acta Physica Polonica A **118**(5), 867 (2010).
[17] R. Guetari, R. Bez, A. Belhadj, K. Zehani, A. Bezergheanu, N. Mliki, L. Bessais, and C. B. Cizmas, J. Alloy Compd. **588**(5), 64 (2014).
[18] S. K. Banerjee, Phys. Lett. **12**, 16 (1964).
[19] R. Skomski and J. M. D. Coey, *Permanent Magnetism* (Institute of Physics, Bristol, 1999).
[20] N. R. Ram, M. Prakash, U. Naresh, N. S. Kumar, T. S. Sarmash, T. Subbarao, R. J. Kumar, G. R. Kumar, and K. C. B. Naidu, J. Supercond. Nov. Magn. **31**, 1971 (2018).